# Analysis of Hop-Distance Relationship in Spatially Random Sensor Networks

Serdar Vural
Department of Electrical and Computer Engineering
The Ohio State University
Columbus, OH 43210
vurals@ece.osu.edu

Eylem Ekici
Department of Electrical and Computer Engineering
The Ohio State University
Columbus, OH 43210
ekici@ece.osu.edu

## ABSTRACT

In spatially random sensor networks, estimating the Euclidean distance covered by a packet in a given number of hops carries a high importance for various other methods such as localization and distance estimations. The inaccuracies in such estimations motivate this study on the distribution of the Euclidean distance covered by a packet in spatially random sensor networks in a given number of hops. Although a closed-form expression of distance distribution cannot be obtained, highly accurate approximations are derived for this distribution in one dimensional spatially random sensor networks. Using statistical measures and numerical examples, it is also shown that the presented distribution approximation yields very high accuracy even for small number of hops. A discussion on how these principles can be extended to the analysis of the same problem in two dimensional networks is also provided.

## Categories and Subject Descriptors

G.3 [**Probability and Statistics**]: Distribution functions; G.1 [**Numerical Analysis**]: Integral Equations; J.2 [**Physical Sciences and Engineering**]

## General Terms

Theory, Experimentation

## Keywords

Sensor Networks, Probability Distribution, Hop Distance, Euclidean Distance, Multihop Propagation

## 1. INTRODUCTION

The Euclidean distance between two nodes in a sensor network can be measured in various ways, such as using the coordinates of the nodes. When the coordinate information is not available or the coordinates cannot be computed, other methods are needed to estimate the distance. A candidate metric for indicating how far away one sensor is from another is the hop distance between the sensors. For networks in which sensor positions are deterministic, the relation between the hop distance and the Euclidean distance can be obtained using simple geometric and algebraic calculations. However, in the case of spatially random networks, the randomness of sensor positions creates random inter-sensor distances. Hence, the Euclidean distance of a hop becomes a random variable. Therefore, relating Euclidean distances with hop distances needs to be accomplished by means of a stochastic study.

Using the hop distance between sensors to obtain distance estimations is a technique applied to position estimation [6], [5]. An average size of one hop is estimated using hop distances to a number of landmarks. The average one hop distance is then used to estimate the Euclidean distances of sensors to the landmarks. In order to obtain approximate node locations, trilateration is performed using these distance estimates. Hop-TERRAIN algorithm in [7] finds the number of hops from a node to each of the anchors nodes in a network and then multiplies this hop count by a shared metric (average hop distance) to estimate the range between the node and each anchor. The known positions of anchor nodes and these computed ranges are used to perform a triangulation to obtain estimated node positions. The problematic issues in these schemes is their sensitivity to the accuracy of the initial position estimates, the magnitude of errors in the range estimates, and the fraction of anchor nodes.

Relating hop distance with Euclidean distance could be used by schemes that require distance estimations without localization of sensors [4], [8]. The *maximum Euclidean distance* that can be attained for a given number of hops can be used to find approximate boundaries of regions where sensor nodes are estimated to exist. Nagpal et al. [4] use the hop distances of sensor nodes from one or more designated sources in order to obtain estimates of inter-sensor Euclidean distances which are used to locate sensor positions. The use of the maximum communication range of a sensor node as the expected distance of a single hop results in errors in estimations. This is due to the fact that the distance to the furthest node is not necessarily equal to communication range and changes according to node density.

The simulation study in [8] has shown that sensors that


*MobiHoc'05,* May 25–27, 2005, Urbana-Champaign, Illinois, USA.

are at particular hop distances from two sources in a two dimensional dense sensor network can be grouped according to these hop distances. Furthermore, the groups are found to be confined within well-defined regions. The boundaries between regions are formed by those sensors that are maximally distant from the sources. However, for a given hop distance from a source, the distance of the boundary sensors from the source node is not a scalar multiple of the communication range. Additionally, the locations of boundary sensors are not deterministic. Therefore, the distribution of the maximum distance of for a given hop distance from sources must be used to determine possible boundary locations.

In a two dimensional sensor network, the Euclidean distance of the farthest sensor that can be reached in a given number of hops from a reference point changes with the direction. This gives rise to the conclusion that the *distribution* of the maximum Euclidean distance for a certain number of hops on a line is a key element for inspecting the more general two dimensional case. As many sensor networks are randomly deployed, such an analysis involves probability density function of Euclidean distances. Furthermore, results obtained for one dimensional multi-hop distribution can be directly applied to vehicular networks [3]. Cheng and Robertazzi [1] derive the probability distribution function of a single hop maximal distance in a one dimensional network. In this study, the expected value of the single hop maximal distance is used for the purpose of determining the expected number of broadcast cycles formed before broadcast percolation ceases. In their study, it is also claimed that this expected distance value is true for any single hop. Although the inter-dependency of single hop distances is mentioned, no results are derived for the probability distribution function of the maximal Euclidean distance for a given hop distance.

In this paper, we analyze the distribution of the maximum Euclidean distance for a given hop distance in one dimension. The theoretical expressions for the *expectation* and the *standard deviation* of Euclidean distance are presented. Since these expressions are computationally costly, efficient approximation methods are proposed. Furthermore, the similarity between the distribution of the multi-hop distance and a Gaussian distribution is evaluated using their *kurtosis* values [2]. We also determine the mean square error between a Gaussian distribution and the distance distribution so as to illustrate their similarity. Furthermore, we provide a discussion on how maximal distances are created in two dimensional networks.

The remainder of the paper is organized as follows: In Section 2, the analysis in one dimensional networks is introduced in more detail. In Sections 2.1 and 2.2, theoretical expressions and approximation equations along with their derivations are introduced respectively. The kurtosis of a single hop distance is approximated in Section 3.2, and the method to obtain an approximation to the kurtosis of the multi-hop distance is derived in Section 3.3. In Section 4, numerical examples are provided for the comparison of the approximation, experimental, and theoretical results. In Section 5, a discussion of the two dimensional problem is presented. Finally, section 6 concludes the paper.

# 2. ONE-DIMENSIONAL ANALYSIS

One dimensional analysis of the distribution of the maximal Euclidean distance for multi-hops is crucial for analyzing 2D maximal distance distributions. In this study, the sensor nodes are uniformly distributed and are assumed to have no mobility and no node failure. It is further assumed that all sensor nodes have the same fixed communication range R and nodes can receive every packet within their communication range.

The total multi-hop maximal distance is the sum of the individual maximal distances taken at each of the hops. The following definitions are used throughout the study:

*Single-hop-distance*: The maximum possible distance covered in a single hop.

*Multi-hop-distance*: The maximum possible distance covered in multiple hops.

For determining each of the single-hop distances that add up to construct a multi-hop distance, the sensor at the maximum distance to the transmitting node is considered. In order to evaluate the probability distribution of the multi-hop distance, the expected value and the standard deviation of the total distance are calculated. The similarity of the Gaussian distribution and the distribution of the multi-hop distance is inspected by determining the kurtosis of the obtained multi-hop distribution.

## 2.1 Theoretical distribution expressions

### 2.1.1 Probability distribution function for single-hop-distance

In the study of Cheng and Robertazzi [1], a stochastic modeling of broadcast percolation in one-dimension is inspected and the pdf of the single-hop-distance is obtained.

***Definition:*** $\mathbf{r_i}$: The distance of the point $P_i$ at the furthest location to the previous point $P_{i-1}$ at hop $i$ is denoted by $\mathbf{r_i}$, where $\mathbf{r_i} \leq R$ for all $i = 1, 2, 3, \cdots$.

***Definition:*** $\mathbf{r_{e_{i-1}}}$: The length of the *vacant* segment from the point $P_i$ to the location R away from the point $P_{i-1}$ at the same direction, where $\mathbf{r_{e_i}} \leq R$ for all $i = 1, 2, 3, \cdots$.

The pdf of $\mathbf{r_i}$ at hop $i$ is computed in [1]:

$$f_{\mathbf{r_i}}(r_i) = \frac{\lambda e^{-\lambda(R-r_i)}}{1 - e^{-\lambda\left(R-r_{e_{i-1}}\right)}}, \tag{1}$$

where node density is denoted by $\lambda$ and the following is always true:

$$\mathbf{r_{e_i}} + \mathbf{r_i} = R.$$

The random variables $\mathbf{r_i}$ and $\mathbf{r_{e_i}}$ for $i = 1, 2, 3, \cdots, N$ are shown in Figure 2.1.2.

The pdf of the vacant region $\mathbf{r_{e_i}}$ can easily be derived from Equation 1 since distance $\mathbf{r_i}$ and the vacancy $\mathbf{r_{e_i}}$ sum up to the constant scalar R. Hence $f_{\mathbf{r_{e_i}}}(r_{e_i}) = f_{\mathbf{r_i}}(R - r_{e_i})$ and the following pdf for $r_{e_i}$ is obtained:

$$f(r_{e_i}) = \frac{\lambda e^{-\lambda r_{e_i}}}{1 - e^{-\lambda\left(R-r_{e_{i-1}}\right)}} \tag{2}$$

From Equations 1& 2, the dependency of the distribution of hop $i$ on the distance at hop $i-1$ is obvious.

### 2.1.2 Probability distribution function for multi-hop-distance

The pdf of $\mathbf{r_{e_i}}$ is dependent on $\mathbf{r_{e_{i-1}}}$ as observed in Equation 2. This dependency between consecutive single-hop-

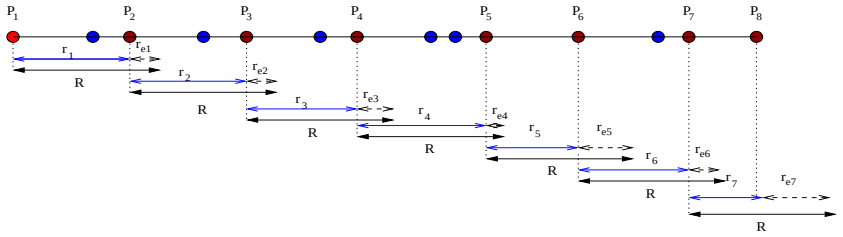


**Figure 1:** ***Linear broadcast propagation in one direction of the source $P_1$. Nodes $P_2$,$P_3$,$P_4$,... are the furthest sensors that receive the broadcast packet at the corresponding hops.***

distances is also mentioned in [1], but the pdf of multi-hop-distance is not derived. The probability distribution of the multi-hop-distance can be written as follows:

$$\begin{aligned} f_{\mathbf{d_N}}(d_N) &= f_{\mathbf{d_{e_N}}}(R - d_N) \\ f_{\mathbf{d_{e_N}}}(d_e) &= \int_0^R \int_0^{R-r_{e_1}} \dots \int_0^{R-r_{e_{N-1}}} \frac{\lambda e^{-\lambda r_{e_N}}}{1 - e^{-\lambda R - r_{e_{N-1}}}} \\ &\quad \dots \frac{\lambda e^{-\lambda r_{e_2}}}{1 - e^{-\lambda R - r_{e_1}}} \frac{\lambda e^{-\lambda r_{e_1}}}{1 - e^{-\lambda R}} dr_{e_N} \dots dr_{e_2} dr_{e_1}, \end{aligned} \tag{3}$$

where $\mathbf{d_N}$ is a random variable for the multi-hop-distance in $N$ hops and $\mathbf{d_{eN}}$ is the sum of the N vacant lengths $\mathbf{r_{e_i}}$ for $i = 1, 2, ..., N$:

$$\mathbf{d_{eN}} = \sum_{i=1}^{N} \mathbf{r_{e_i}}.$$

In Equation 3, $f_{\mathbf{d_N}}(d_N) = f_{\mathbf{d_{e_N}}}(R - d_N)$ holds since

$$\mathbf{d_N} = NR - \sum_{i=1}^{N} \mathbf{r_{e_i}}. \tag{4}$$

and $NR$ is a deterministic quantity.

As observed in Equation 3, the distribution of the multi-hop-distance is a nested integral which cannot be reduced to a closed-form expression. Furthermore, its numerical solution is impractical and costly.

Apart from using the pdf, a distribution can be studied using its mean and its standard deviation. Although the theoretical expressions for these two measures are also computationally costly, approximation methods are proposed as will be explained in Section 2.2.

The pdf of the vacant region $\mathbf{r_{e_i}}$ has an analytically easier form than that of $\mathbf{r_i}$ for the purpose of calculating its expectation and its variance. Therefore, the expected multi-hop-distance of N hops $E[\mathbf{d_N}]$ is calculated by finding the expectation of $\mathbf{d_{e_N}}$ and subtracting this quantity from N times the communication range R as stated in Equation 4.

***Proposition***: The variance of the multi-hop-distance $\mathbf{d_N}$ is equal to the variance of total of the N consecutive vacant region lengths, $\mathbf{d_{e_N}}$. Hence:

$$\sigma^2_{\mathbf{d_N}} = \sigma^2_{\mathbf{d_{e_N}}} \tag{5}$$

PROOF. The variance of $\mathbf{d_N}$ can be written as:

$$\begin{aligned} E[(\mathbf{d_N} - \overline{d_N})^2] &= E[(NR - \mathbf{d_{e_N}} - \overline{d_N})^2] \\ &= E[(NR - \mathbf{d_{e_N}})^2 - 2\overline{d_N}(NR - \mathbf{d_{e_N}}) + \overline{d_N}^2] \\ &= E[(NR)^2 - 2NR\mathbf{d_{e_N}} + \mathbf{d_{e_N}}^2 \\ &\quad -2\overline{d_N}NR + 2\overline{d_N}\mathbf{d_{e_N}} + \overline{d_N}^2] \\ &= (NR)^2 - 2NR\overline{d_{e_N}} + E[\mathbf{d_{e_N}}^2] - 2\overline{d_N}NR \\ &\quad +2\overline{d_N}\,\overline{d_{e_N}} + \overline{d_N}^2 \\ &= (NR)^2 - 2NR\overline{d_{e_N}} + E[\mathbf{d_{e_N}}^2] \\ &\quad -2(NR - \overline{d_{e_N}})NR + 2(NR - \overline{d_{e_N}})\overline{d_{e_N}} \\ &\quad +(NR)^2 - 2\overline{d_{e_N}}NR + \overline{d_{e_N}}^2 \\ &= E[\mathbf{d_{e_N}}^2] - \overline{d_{e_N}}^2 \\ \sigma^2_{\mathbf{d_N}} &= \sigma^2_{d_{\mathbf{e_N}}}, \end{aligned}$$

where $\overline{d_N}$ is the mean of $d_N$ and $\overline{d_{e_N}}$ is the mean of $d_{e_N}$. Hence, the variance of $\mathbf{d_N}$ can be found by determining the variance of $\mathbf{d_{e_N}}$.

□

The expressions for the expected value of the multi-hop-distance and that of the variance can be written as follows:

$$\begin{aligned} E[\mathbf{d_N}] &= \int_0^R \int_0^{R-r_{e_1}} \dots \int_0^{R-r_{e_{N-1}}} \frac{d_N \lambda e^{-\lambda r_{e_N}}}{1 - e^{-\lambda R - r_{e_{N-1}}}} \\ &\quad \dots \frac{\lambda e^{-\lambda r_{e_2}}}{1 - e^{-\lambda R - r_{e_1}}} \frac{\lambda e^{-\lambda r_{e_1}}}{1 - e^{-\lambda R}} dr_{e_N} \dots dr_{e_2} dr_{e_1} \end{aligned} \tag{6}$$

$$\begin{aligned} \sigma^2_{\mathbf{d_N}} &= \int_0^R \int_0^{R-r_{e_1}} \dots \int_0^{R-r_{e_{N-1}}} \frac{(d_N - \overline{d_N})^2 \lambda e^{-\lambda r_{e_N}}}{1 - e^{-\lambda R - r_{e_{N-1}}}} \\ &\quad \dots \frac{\lambda e^{-\lambda r_{e_2}}}{1 - e^{-\lambda R - r_{e_1}}} \frac{\lambda e^{-\lambda r_{e_1}}}{1 - e^{-\lambda R}} dr_{e_N} \dots dr_{e_2} dr_{e_1}, \end{aligned} \tag{7}$$

where $\mathbf{d_N}$ is given in Equation 4 and $\overline{d_N} = E[\mathbf{d_N}]$. Equations 6 and 7 are nested integrals like the pdf expression in Equation 3. However, they can be approximated as will be shown in the next section.

## 2.2 Approximations of $1^{st}$ and $2^{nd}$ order statistics

Approximations for the expectation and standard deviation of single-hop-distance and multi-hop-distance are required due their computationally costly theoretical expressions.

### 2.2.1 Expected single-hop-distance

In [1], $\mathbf{r_i}$ is replaced by its expectation $E[\mathbf{r_i}]$ and the equivalence of the expected single-hop-distances is assumed to be

$$E[\mathbf{r_i}] = E[\mathbf{r_{i-1}}] = \overline{r}. \tag{8}$$

In this study, Equation 8 is used to derive closed form equations of statistics of the single-hop-distance, which in turn prove to be handy in calculating the statistics of the multi-hop-distance. Equation 8 is extended so as to:

- make a proposal for the expected multi-hop-distance,
- obtain the second moments of single-hop-distance and multi-hop-distance, and obtain higher order statistics for investigating Gaussianity of single-hop-distance in Section 3.2.

The following proposition is provided and proved in [1], which is used for obtaining the expected value of a single-hop-distance.

***Proposition***: The expected length of the vacant region $\mathbf{r_{e_i}}$ at hop $i$ is given as [1]:

$$E[\mathbf{r_{e_i}}] = \frac{1 - e^{-\lambda\left(R - r_{e_{i-1}}\right)}\left(1 + \lambda\left(R - r_{e_{i-1}}\right)\right)}{\lambda\left(1 - e^{-\lambda\left(R - r_{e_{i-1}}\right)}\right)} \tag{9}$$

By the definition of a vacant region $\mathbf{r_{e_i}}$ and using Equation 8, the expected distance at hop $i$ is given as:

$$E[\mathbf{r_i}] = \overline{r} = R - E[\mathbf{r_{e_i}}]. \tag{10}$$

Replacing $\mathbf{r_i}$ and $\mathbf{r_{i-1}}$ with their expectations and using Equation 8, the righthand side of Equation 10 can be substituted in Equation 9. As a result, the following expression for finding the approximation of the expected single-hop-distance is obtained:

$$\ln\left(1 - \frac{\lambda\overline{r}}{\lambda R - \lambda\overline{r} - 1}\right) = \lambda\overline{r} \tag{11}$$

Expression 11 is an implicit expression. Therefore, the values of $\overline{r}$ are obtained numerically.

### 2.2.2 Variance of single-hop-distance

Similar to the derivation of the expression for the expected single-hop-distance, the expression for the standard deviation of single-hop-distance can be obtained by using an analytically easier calculation of the variance of $\mathbf{r_e}$, rather than directly calculating the variance of $\mathbf{r}$. Since $\mathbf{d_N} = \mathbf{r}$ for $N = 1$, using Equation 5, the following relation is obtained:

$$\sigma_{\mathbf{r}}^2 = \sigma_{\mathbf{r_e}}^2 \tag{12}$$

So the variance of single-hop-distance becomes:

$$\sigma_{\mathbf{r}}^2 = \sigma_{\mathbf{r_e}}^2 = E[\mathbf{r_e^2}] - \overline{r_e}^2 = E[\mathbf{r_e^2}] - (R - \overline{r})^2 \tag{13}$$

The second moment of $\mathbf{r_e}$ in Equation 13 can be found similar to the way outlined in [1] for finding $E[\mathbf{r_e}]$ and is obtained as follows:

$$\begin{aligned} E[\mathbf{r_{e_i}}^2] &= -\frac{e^{-\lambda\left(R - r_{e_{i-1}}\right)}}{1 - e^{-\lambda\left(R - r_{e_{i-1}}\right)}}\left(R - r_{e_{i-1}}\right)^2 \\ &\quad -\frac{e^{-\lambda\left(R - r_{e_{i-1}}\right)}}{1 - e^{-\lambda\left(R - r_{e_{i-1}}\right)}}\frac{2}{\lambda}\left(R - r_{e_{i-1}}\right) \\ &\quad +\frac{1}{1 - e^{-\lambda\left(R - r_{e_{i-1}}\right)}}\left\{\frac{2}{\lambda^2} - \frac{2}{\lambda^2}e^{-\lambda\left(R - r_{e_{i-1}}\right)}\right\}. \end{aligned} \tag{14}$$

In Equation 14, $\mathbf{r_i}$ and $\mathbf{r_{e_i}}$ are replaced by their expectation and Equation 8 is used to claim that $\mathbf{r_{e_i}} = \mathbf{r_{e_{i-1}}} \equiv R - \overline{r}$. Equation 10 is then substituted in Equation 14. Hence, $R - \mathbf{r_{e_{i-1}}} = \mathbf{r_{i-1}} \approx \mathbf{r_i} \equiv \overline{r}$ and the second moment can be written as:

$$E[\mathbf{r_e}^2] = \frac{-\overline{r}^2 e^{-\lambda\overline{r}} - \frac{2}{\lambda}\overline{r}e^{-\lambda\overline{r}} + \frac{2}{\lambda^2} - \frac{2}{\lambda^2}e^{-\lambda\overline{r}}}{1 - e^{-\lambda\overline{r}}}. \tag{15}$$

Substituting Equation 15 into Equation 13, the variance of the single-hop-distance can be found.

In Equation 15, a much stronger assumption than Equation 8 is required to claim that the second order moments of all single-hop-distances are equal, that is, $E[\mathbf{r_{e_i}}^2] = E[\mathbf{r_e}^2]$. In order to determine higher order moments of a single-hop-distance and to investigate the statistics of the multi-hop-distance, it is assumed that ***single-hop-distances are identically distributed but not independent.*** This assumption is also used in Section 3.

### 2.2.3 Expected value and variance of multi-hop distance

As shown in Equation 4, multi-hop-distance is the sum of single-hop-distances. Since expectation is a linear operator, the expectation of a multi-hop-distance is equal to the sum of the expectations of the single-hop-distances. Equation 8 claims that the expected value of any single-hop-distance is $\overline{r}$. Hence,

$$E[\mathbf{d_N}] = E\left[\sum_{i=1}^{N}\mathbf{r_i}\right] = N\overline{r}. \tag{16}$$

Then, the standard deviation of the multi-hop-distance for N hops can be derived as follows:

$$\begin{aligned} E\left[\left(\mathbf{d_N} - \overline{d_N}\right)^2\right] &= E\left[\left(\left(\sum_{i=1}^{N}\mathbf{r_i}\right) - \left(\sum_{i=1}^{N}\overline{r_i}\right)\right)^2\right] \\ &= E\left[\left(\sum_{i=1}^{N}\mathbf{r_i}\right)^2 - 2\left(\sum_{i=1}^{N}\mathbf{r_i}\right)\left(\sum_{i=1}^{N}\overline{r_i}\right)\right] \\ &\quad +E\left[\left(\sum_{i=1}^{N}\overline{r_i}\right)^2\right] \\ &= E\left[\left(\sum_{i=1}^{N}\mathbf{r_i}\right)^2\right] - N^2\overline{r}^2 \end{aligned} \tag{17}$$

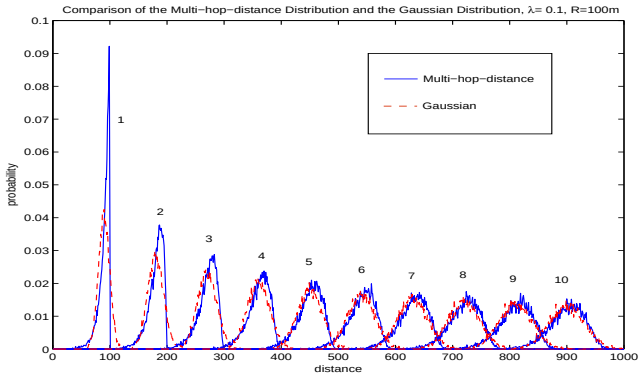


**Figure 2:** ***Distributions of the multi-hop-distances for*** $N = 1, 2, 3, ..., 10$ ***and the corresponding experimental Gaussian distributions. R=100***

The term $E\left[\left(\sum_{i=1}^{N} \mathbf{r_i}\right)^2\right]$ can be calculated by Equations 29 and 30.

# 3. GAUSSIANITY OF THE SINGLE-HOP-DISTANCE AND MULTI-HOP-DISTANCE DISTRIBUTIONS

Multi-hop-distance is the sum of single-hop-distances and the single-hop-distances are assumed to be identically distributed. Although single-hop-distances are not independent and the number of single-hop-distances that sum up to form a multi-hop-distance is not infinitely-many, the distribution curves for increasing number of hops get more Gaussian-like as illustrated in Figure 3.

In Figure 3, experimentally obtained distributions of the multi-hop-distance $\mathbf{d_N}$ is shown for different number of hops, $N = 1, 2, 3, ..., 10$. For each $N$, there is a distribution plot of $\mathbf{d_N}$ centered at its mean value $E[\mathbf{d_N}]$. The experimental Gaussian distributions of corresponding means and standard deviations are also plotted for each of these multi-hop-distance distribution plots. The distribution of the multi-hop-distance approaches to the corresponding Gaussian distribution as the number of hops $N$ becomes larger.

The increasing similarities between the two distributions suggest that *the multi-hop distance distribution can be approximated by a corresponding Gaussian one*, which is only described by its mean and variance. In Equations 16 and 17 effective ways of approximating the mean and variance of multi-hop-distance distribution are presented. However, a quantitative method to test the Gaussianity of multi-hop-distance is required. Section 3.1 introduces such a measure called *kurtosis*, and Sections 3.2 and 3.3 explain how the kurtosis values of single-hop-distance and multi-hop-distance distributions are determined, respectively.

## 3.1 Kurtosis as a measure of Gaussianity

Kurtosis is a statistical measure of the peakedness of a probability distribution. The kurtosis of a random variable $\mathbf{x}$ is defined as:

$$kurt\,(\mathbf{x}) = \frac{E[(\mathbf{x} - \overline{x})^4]}{E[(\mathbf{x} - \overline{x})^2]^2}. \tag{18}$$

Equation 18 could be defined as the ratio of the fourth order central moment and the square of the variance, i.e., it is a ratio of central moments. In addition to measuring peakedness, kurtosis is also used to determine the Gaussianity of a probability distribution [2].

Another definition of kurtosis is *"kurtosis excess"*, which is 3 less than the general kurtosis expression (Equation 18). For a normal distribution, the kurtosis is equal to 3 and the kurtosis excess of a normal distribution is zero. Hence, *in order to obtain a more Gaussian-like distribution, the absolute value of kurtosis-excess should be minimized.* In the remainder of the paper, the term *kurtosis* is used to refer to *kurtosis excess.*

## 3.2 Gaussianity of the single-hop-distance distribution

In this part of our study, the Gaussianity of the pdf of the single-hop-distance $\mathbf{r}$ is inspected. The kurtosis expression is found to be dependent on the changes in the node density $\lambda$, communication range R, and the number of hops N. Equation 18 is expanded and the variable $\mathbf{x}$ is replaced by $\mathbf{r}$ to obtain the kurtosis of the single-hop-distance.

$$kurt\,(\mathbf{r}) = \frac{E[\mathbf{r^4}] - 4E[\mathbf{r^3}]E[\mathbf{r}] + 6E[\mathbf{r^2}]E[\mathbf{r}]^2 - 3E[\mathbf{r}]^4}{(E[\mathbf{r^2}] - E[\mathbf{r}]^2)^2} \tag{19}$$

In Equation 19, the kurtosis expression involves the fourth and the third order moments of a single-hop-distance. In this section, any single-hop-distance is referred as $\mathbf{r}$ and any single-hop vacant region as $\mathbf{r_e}$, without using a subscript $i$ to denote the hop count. As it was the case for the second order moment, calculating the third and the fourth moments of the vacant length $\mathbf{r_e}$ is much easier than calculating the corresponding moments of the distance $\mathbf{r}$. The moments of the vacant region $\mathbf{r_e}$ in a single step can be used to obtain the moments of the single-hop-distance $r$. This is due to the fact that there is only a scalar difference between these two random variables as $\mathbf{r_e} + \mathbf{r} = R$. The relationship between the moments of $\mathbf{r_e}$ and $\mathbf{r}$ is as follows:

$$E[\mathbf{r}^3] = R^3 - 3R^2(R - E[\mathbf{r}]) + 3RE[{\mathbf{r_e}}^2] - E[{\mathbf{r_e}}^3] \tag{20}$$

$$E[\mathbf{r}^4] = R^4 - 4R^3(R - E[\mathbf{r}]) + 6R^2E[{\mathbf{r_e}}^2] - 4RE[{\mathbf{r_e}}^3] + E[{\mathbf{r_e}}^4] \tag{21}$$

Using our assumption that single-hop-distances are identically distributed, $E[{\mathbf{r_{e_i}}}^j] = E[{\mathbf{r_e}}^j]$. The expressions $E[{\mathbf{r_{e_i}}}^3]$ and $E[{\mathbf{r_{e_i}}}^4]$ are calculated as:

$$\begin{aligned} E[{\mathbf{r_{e_i}}}^3] = {} & \frac{e^{-\lambda(R-r_{e_{i-1}})}}{1 - e^{-\lambda(R-r_{e_{i-1}})}} \left(-(R - r_{e_{i-1}})^3\right) \\ & - \frac{e^{-\lambda(R-r_{e_{i-1}})}}{1 - e^{-\lambda(R-r_{e_{i-1}})}} \frac{3}{\lambda}(R - r_{e_{i-1}})^2 \\ & - \frac{e^{-\lambda(R-r_{e_{i-1}})}}{1 - e^{-\lambda(R-r_{e_{i-1}})}} \left(\frac{6}{\lambda^2}(R - r_{e_{i-1}}) + \frac{6}{\lambda^3}\right) \\ & + \frac{6}{\lambda^3\left(1 - e^{-\lambda(R-r_{e_{i-1}})}\right)} \end{aligned} \tag{22}$$

$$
\begin{aligned}
E[\mathbf{r_{e_i}}^4] &= \frac{e^{-\lambda(R-r_{e_{i-1}})}}{1-e^{-\lambda(R-r_{e_{i-1}})}}\left(-(R-r_{e_{i-1}})^4\right) \\
&\quad -\frac{e^{-\lambda(R-r_{e_{i-1}})}}{1-e^{-\lambda(R-r_{e_{i-1}})}}\frac{4}{\lambda}(R-r_{e_{i-1}})^3 \\
&\quad -\frac{e^{-\lambda(R-r_{e_{i-1}})}}{1-e^{-\lambda(R-r_{e_{i-1}})}}\left(\frac{12}{\lambda^2}(R-r_{e_{i-1}})^2+\frac{24}{\lambda^4}\right) \\
&\quad +\frac{1}{1-e^{-\lambda(R-r_{e_{i-1}})}}\left(\frac{24}{\lambda^4}-\frac{24}{\lambda^3}(R-r_{e_{i-1}})\right)
\end{aligned} \tag{23}
$$

After deriving $E[\mathbf{r_{e_i}}^j]$, where $j = 1, 2, 3, \cdots$, the variables $\mathbf{r_{e_i}}$ and $\mathbf{r_{e_{i-1}}}$ are both replaced by $\mathbf{r_e}$. Similarly, $\mathbf{r_i}$ and $\mathbf{r_{i-1}}$ are both changed to be $\mathbf{r}$. In the same way, the third and the fourth moments of $\mathbf{r_e}$ can be found as follows:

$$
\begin{aligned}
E[\mathbf{r_e}^3] &= \frac{e^{-\lambda\overline{r}}}{1-e^{-\lambda\overline{r}}}\left(-\overline{r}^3-\frac{3}{\lambda}\overline{r}^2-\frac{6}{\lambda^2}\overline{r}-\frac{6}{\lambda^3}\right) \\
&\quad +\frac{6}{\lambda^3\left(1-e^{-\lambda\overline{r}}\right)} \qquad (24) \\
E[\mathbf{r_e}^4] &= \frac{e^{-\lambda\overline{r}}}{1-e^{-\lambda\overline{r}}}\left(-\overline{r}^4-\frac{4}{\lambda}\overline{r}^3-\frac{12}{\lambda^2}\overline{r}^2-\frac{24}{\lambda^4}\right) \\
&\quad +\frac{1}{1-e^{-\lambda\overline{r}}}\left(\frac{24}{\lambda^4}-\frac{24}{\lambda^3}\overline{r}\right) \qquad (25)
\end{aligned}
$$

Using the expected single-hop-distance $r$ of Equation 8, Equations 24 and 25 are evaluated to get the third and the fourth moments of $\mathbf{r_e}$, respectively. The results are used in Equations 20 and 21 to get the third and fourth moments of $\mathbf{r}$, respectively. Using the third moment (Equation 20), the fourth moment (Equation 21), the second moment (Equations 13 and 15) and the expected single-hop-distance (Equation 8), Equation 19 is evaluated to obtain the kurtosis of the single-hop-distance.

## 3.3 Gaussianity of the distribution of multi-hop-distance $d_N$

In this section, the Gaussian character of the multi-hop-distance destination is investigated. Using the approximation for the expected single-hop-distance, Equation 8, and the definition of kurtosis, Equation 18, the expression to compute the kurtosis of the multi-hop-distance can be obtained as follows:

$$
\begin{aligned}
kurt(\mathbf{d_N}) &= \frac{E[(\mathbf{d_N}-\bar{d_N})^4]}{E[(\mathbf{d_N}-\bar{d})^2]^2} \\
&= \frac{E[(\sum_1^N \mathbf{r_i}-\sum_1^N \bar{r_i})^4]}{E[(\sum_1^N \mathbf{r_i}-\sum_1^N \bar{r_i})^2]^2} \\
&= \frac{E[(\sum_1^N \mathbf{r_i})^4-4(\sum_1^N \mathbf{r_i})^3(\sum_1^N \bar{r_i})]}{E[(\sum_1^N \mathbf{r_i})^2+(\sum_1^N \bar{r_i})^2-2(\sum_1^N \mathbf{r_i})(\sum_1^N \bar{r_i})]} \\
&\quad +\frac{E[6(\sum_1^N \mathbf{r_i})^2(\sum_1^N \bar{r_i})^2]}{E[(\sum_1^N \mathbf{r_i})^2+(\sum_1^N \bar{r_i})^2-2(\sum_1^N \mathbf{r_i})(\sum_1^N \bar{r_i})]} \\
&\quad -\frac{E[4(\sum_1^N \mathbf{r_i})(\sum_1^N \bar{r_i})^3-(\sum_1^N \bar{r_i})^4]}{E[(\sum_1^N \mathbf{r_i})^2+(\sum_1^N \bar{r_i})^2-2(\sum_1^N \mathbf{r_i})(\sum_1^N \bar{r_i})]}
\end{aligned} \tag{26}
$$

Equation 26 can be simplified by distributing the expectation operations since expectation is a linear operator. The terms like $4\left(\sum_1^N \mathbf{r_i}\right)^3\left(\sum_1^N \bar{r_i}\right)$, where $E[\mathbf{r_i}] = \bar{r_i}$ can also be recognized. In such multiplications, $\left(\sum_1^N \bar{r_i}\right)$ is the sum of the $N$ expected single-hop-distances. Since the sum of expected values is a constant, $\left(\sum_1^N \bar{r_i}\right)$ becomes a scalar multiplier of $E[\left(\sum_1^N \mathbf{r_i}\right)^3]$. In general, the expectation of any term of the form $\left(\sum_1^N \mathbf{r_i}\right)^p\left(\sum_1^N \bar{r_i}\right)^s$, where p and s are some integers and $p, s > 0$, involving $\left(\sum_1^N \bar{r_i}\right)$ as a multiplier, can be evaluated as follows:

$$
E\left[(\sum_1^N \mathbf{r_i})^{\ p}\ (\sum_1^N \bar{r_i})^{\ s}\right] = (\sum_1^N \bar{r_i})^{\ s}\ E\left[(\sum_1^N \mathbf{r_i})^{\ p}\right] \tag{27}
$$

Using Equation 27, Equation 26 can be modified to obtain:

$$
\begin{aligned}
&kurt(d) = \\
&= \frac{E[(\sum_1^N \mathbf{r_i})^4]-4(\sum_1^N \bar{r_i})E[(\sum_1^N \mathbf{r_i})^3]}{E[(\sum_1^N \mathbf{r_i})^2]-2E[(\sum_1^N \mathbf{r_i})](\sum_1^N \bar{r_i})+(\sum_1^N \bar{r_i})^2} \\
&\quad +\frac{6(\sum_1^N \bar{r_i})^2E[(\sum_1^N \mathbf{r_i})^2]-4(\sum_1^N \bar{r_i})^3E[(\sum_1^N \mathbf{r_i})]}{E[(\sum_1^N r_i)^2]-2E[(\sum_1^N \mathbf{r_i})](\sum_1^N \bar{r_i})+(\sum_1^N \bar{r_i})^2} \\
&\quad +\frac{(\sum_1^N \bar{r_i})^4}{E[(\sum_1^N \mathbf{r_i})^2]-2E[(\sum_1^N \mathbf{r_i})](\sum_1^N \bar{r_i})+(\sum_1^N \bar{r_i})^2}
\end{aligned} \tag{28}
$$

In Equation 28, the terms in the form of $E\left[(\sum_1^N \mathbf{r_i})^j\right]$ for $j = 2, 3, 4$ are calculated as follows: Let $f_j(N)$ be defined as $f_j(N) \equiv E\left[(\sum_1^N \mathbf{r_i})^j\right]$, where $N$ is the hop distance and $j$ is the power term. Then, $f_j(N)$ is computed recursively as:

$$
\begin{aligned}
f_2(N) &= f_2(N-1) + 2(N-1)\overline{r}^2 + E[\mathbf{r}^2] \\
f_3(N) &= f_3(N-1) + 3f_2(N-1)\overline{r} \\
&\quad +3(N-1)\overline{r}E[\mathbf{r}^2] + E[\mathbf{r}^3] \\
f_4(N) &= f_4(N-1) + 4f_3(N-1)\overline{r} \\
&\quad +6f_2(N-1)E[\mathbf{r}^2] \\
&\quad +4(N-1)\overline{r}E[\mathbf{r}^3] + E[\mathbf{r}^4] \qquad (29)
\end{aligned}
$$

The functions $f_j(N)$ can be computed directly for $N = 2$ and $j = 2, 3, 4$:

$$
\begin{aligned}
f_2(2) &= 2E[\mathbf{r}^2] + 2\overline{r}^2 \\
f_3(2) &= 2E[\mathbf{r}^3] + 6E[\mathbf{r}^2]\overline{r} \\
f_4(2) &= 2E[\mathbf{r}^4] + 6E[\mathbf{r}^2]^2 + 8E[\mathbf{r}^3]\overline{r} \qquad (30)
\end{aligned}
$$

The values of the terms like $E\left[(\sum_1^N \bar{r_i})^j\right]$ for $j = 2, 3, 4$ are very easy to compute since there is no random quantity inside the expectation operator. According to Assumption 8, $E[\mathbf{r_i}] = \overline{r_i}$ is simply $\overline{\mathbf{r}}$, for all $i$. Hence, $E\left[(\sum_1^N \bar{r_i})^j\right] = E[(N\overline{r})^j]$ holds. $N\overline{r}$ and the powers of $N\overline{r}$ are deterministic quantities. The expectation of $(\sum_1^N \bar{r_i})^j$ for $j = 1, 2, 3, \cdots$ is then:

$$
E\left[(\sum_1^N \bar{r_i})^j\right] = E\left[(N\overline{r})^j\right] = N^j\overline{r}^j \qquad (31)
$$

Equation 31 and Equation 29 are then used in Equation 28 to get the kurtosis of a multi-hop-distance consisting of $N$ single-hop-distances.

# 4. PERFORMANCE EVALUATION

In this section, the numerical results of theoretical and approximated expressions for distance distributions are introduced. Furthermore, experiments are conducted to seek the validity of our approximations. The expressions that are evaluated are the following:

- Expected single-hop and expected multi-hop distances (Equation 6)
- Standard deviation of single-hop and multi-hop distances (Equation 7)
- Kurtosis of single-hop-distance (Equation 19)
- Kurtosis for multi-hop distance (Equation 28)

First, how our mathematical expressions are used to obtain the graphs to analyze multi-hop-distance and single-hop-distance distributions is described. Then, the theoretical, experimental, and approximation curves are compared. Finally, how the kurtosis graphs reflect the Gaussian behavior of multi-hop-distance distributions is discussed.

## 4.1 Implementations

### 4.1.1 Theoretical Expressions

The maximum number of hops that is implemented for multi-hop-distance case is limited to 5 due to the computational cost of the multi-hop expressions which are in the form of nested integrals. As will be demonstrated in the next section, our approximation methods applied to these expressions are quite accurate.

The theoretical distribution expressions of the expected single-hop-distance and expected multi-hop-distance are implemented according to Equation 6. To find the expected single-hop-distance of a particular hop, say $k$, Equation 6 is evaluated for $N = k$ and $N = k - 1$ separately. The difference of these two results gives the theoretical expectation of the single-hop-distance in hop $k$. Similarly, the theoretical expressions of the standard deviation of single-hop-distance and standard deviation of multi-hop-distance are implemented according to Equation 7. Taking $N = 1$, the standard deviation of the first single-hop-distance is obtained, while for $N > 1$ the standard deviation of multi-hop-distance is found.

The equations for finding the kurtosis of single-hop-distance and the kurtosis of multi-hop-distance are Equation 19 and Equation 28, respectively.

### 4.1.2 Approximation Expressions

The approximation expressions are derived to avoid the computational cost of the theoretical ones. Equation 8, which is the assumption in [1], is used to obtain the expected single-hop-distance and expected multi-hop-distance (Equation 13). Kurtosis of the multi-hop-distance (Equation 29) and the standard deviation of single-hop and multi-hop distances (Equations 16 and 17) are calculated. Kurtosis of single-hop-distance is calculated using Equation 19.

### 4.1.3 Experimental study

In order to evaluate the validity of the theoretical and approximation results, 10000 independent experiments are performed using linear spatially random sensor networks with uniform node density.

## 4.2 Results

### 4.2.1 Expectation and standard deviation of single-hop-distance

In Figure 3, the theoretical value of the expected single-hop-distance $E[\mathbf{r}]$ is found to be approaching to the approximation. The hop distances are found to have a decaying oscillatory character around $E[\mathbf{r}]$. This shows that the approximation in Equation 8 is not accurate for the first few hops and improves for larger hop numbers to match the approximated value. Due to the computational cost of the numerical implementation of the theoretical expressions, the expected distance values for up to five hops is shown in this figure.

In Figure 4(a), the analytical, experimental, and approximated values of the expectation of a single-hop-distance are presented. As it can be observed, the approximated values are very accurate since the curve of the theoretical values is closely matched. The approximated and the theoretical results resemble the experimental results almost perfectly, which shows their validity. Figure 4(b) illustrates the com-

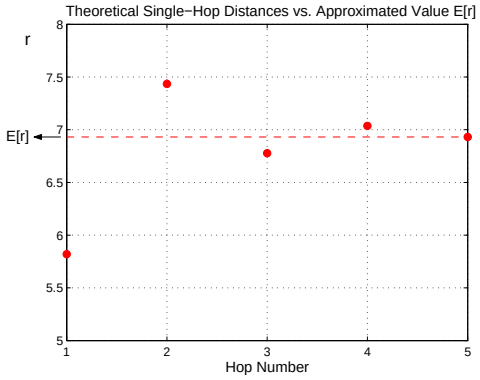


**Figure 3:** ***Comparison of the theoretical values of the single-hop-distances taken at the first five hops with the approximation of a single-hop-distance,*** $E[r]$. ***R=10,*** $\lambda = 0.1$

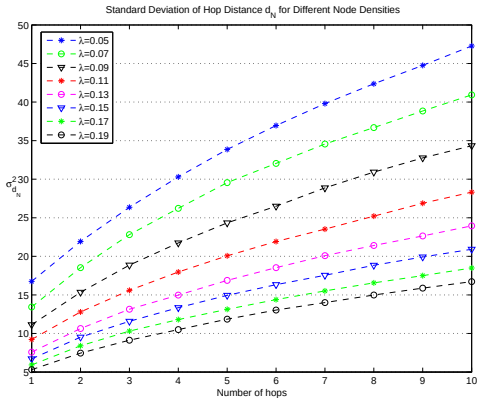


**Figure 6:** ***Experimental values of the standard deviation of the multi-hop-distance with N hops,*** $\sigma_d$***, for*** $N = 1, 2, 3, ..., 10$***, in case of different node densities. R=100***

parison of the analytical, experimental, and approximated values of the standard deviation of a single-hop-distance. As it is the case in Figure 4(a), the approximated and the theoretical results match the experimental results almost perfectly, which demonstrates the success of the approximations and the validity the theoretical expressions for calculating standard deviations.

### 4.2.2 Expectation and standard deviation of multi-hop-distance

In Figure 6, the change in the standard deviation of multi-hop-distance in N hops for changing node density $\lambda$ is shown for $N = 1, 2, 3, ..., 10$. The increase in deviation with decreasing node density is apparent. This shows that the distribution of multi-hop-distance becomes less concentrated around its mean as the node density decreases. This is an expected result since less node density causes more randomness in sensor locations. Another observation in Figure 6 is that the standard deviation curves are not linearly proportional to the number of hops $N$. This is an indication that the *single-hop-distances are not independent*, since the standard deviation of the sum of identically distributed independent random variables is $\sigma_Y = M\sigma_X$, where $X$ is a single random variable and $Y$ is the sum of $M$ identically distributed single random variables. This is also an expected result, since it is known that the distribution of the single-hop-distance in a hop is dependent on the single-hop-distance in the previous hop.

Figure 5(a) shows the change of the mean of a multi-hop-distance for two selected node densities. The results of theoretical, approximated, and experimental implementations are compared. Since the computations of the integral expressions are costly, no larger than N=4 hops is illustrated. As it can be observed, the three results overlap which shows the validity of our approximation for the expected multi-hop-distance value. The mean expected value of multi-hop-distance is found to be linearly proportional to the mean of single-hop-distance as suggested in Equation 16.

Figure 5(b), illustrates the expected distance of N hops, $N = 1, 2, 3, ..., 10$, obtained by experimentation and approximation. In order to present a larger number of hops, theoretical results are not shown in Figure 5(b). The standard deviations $\sigma_{\mathbf{d_N}}$ of the total distance $\mathbf{d_N}$ are shown by using error bars around the expected distance values. The figure shows the results for selected high ($\lambda = 0.2$ *nodes*$/m$) and low ($\lambda = 0.05$ *nodes*$/m$) node densities. The experimental and approximated results are quite similar and they overlap. The linearity of experimental expected distance curves suggests that $E[\mathbf{d_N}]$ is linearly proportional to the number of hops as claimed in Equation 16. The standard deviation values found by Equation 17 and the experimental values are also quite similar and they appear to be represented by a single deviation error bar. The increase in deviation with decreasing node density and increasing number of hops can be observed in Figure 5(b), which was also shown in more detail in Figure 6.

### 4.2.3 Gaussianity of multi-hop-distance

The kurtosis values of a multi-hop-distance can be experimentally shown for a large number of hops. In Figure 7, the experimental kurtosis is shown as a function of number of hops $N$ in case of a node density of $\lambda = 0.5$ nodes/m and a communication range of $R = 100m$. The function and hence the non- Gaussianity has a decreasing character with increasing number of hops, yet it then, say after $N = 50$ hops, settles within a range of [0 0.2]. This fluctuation seems to cease in amplitude for considerably large hop counts.

In Figure 8, it can be observed that the behaviors of the kurtosis curves with changing node density $\lambda$ and changing number of hops $N$ are similar in experiments and approximation results. Generally, it is observed that increasing number of hops increases the Gaussianity of the multi-hop-distance. Furthermore, for lower node densities, the Gaussianity increases. This is an expected result, since Gaussian distribution is the most "random" distribution among those distributions having the same mean and standard deviation and for low densities the distribution of nodes present a more random character. For large densities, the number of nodes found per unit area is close to the overall node density, whereas for smaller node densities this is more unlikely. Figure 8(a) illustrates how the kurtosis, hence the Gaussianity of the multi-hop-distance is affected by the change in the node density. This figure is obtained using Equation 27, hence it shows approximated values. Figure 8(b) illustrates the effect of node density on the Gaussianity of the

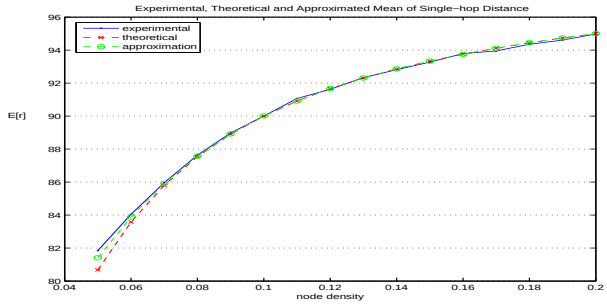


(a) *Expected single-hop-distance* $E[r]$, $R$=100

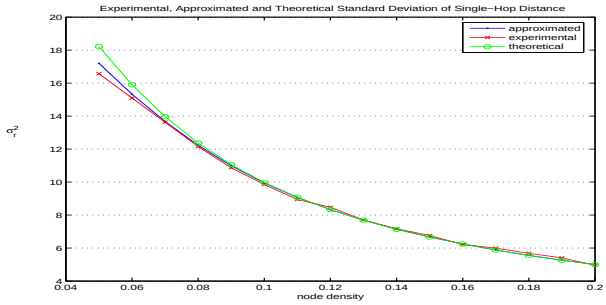


(b) *Standard deviation in single-hop-distance* $\sigma_r^2$, $R$=100

**Figure 4: Comparison of Theoretical, Approximated and Experimental Results for the expectation and standard deviation of single-hop-distance for Changing Node Density**

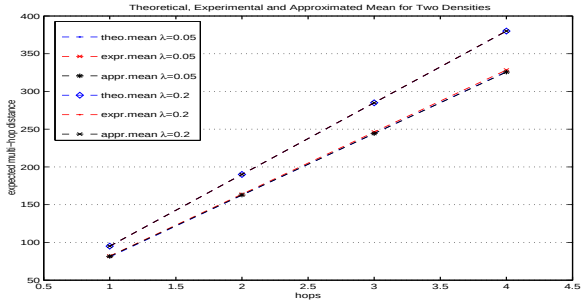


(a) *Experimental, Approximated and Theoretical,* $N = 1, 2, 3, 4$, $R = 100$, $\lambda = 0.05 nodes/m$ *and* $0.2 nodes/m$

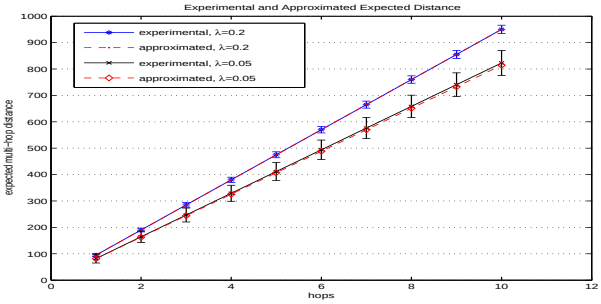


(b) *Experimental and Approximated,* $N = 1, 2, 3, ..., 10$, $R = 100$, $\lambda = 0.05 nodes/m$ *and* $0.2 nodes/m$

**Figure 5: Comparison of Theoretical, Approximated and Experimental Results for the expectation and standard deviation of multi-hop-distance**

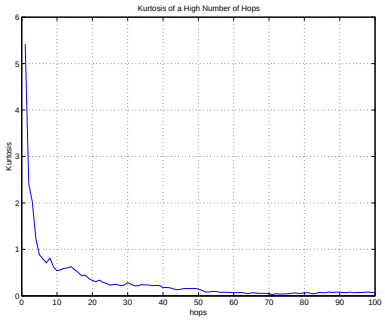


**Figure 7:** ***Experimental values of the kurtosis of the multi-hop-distance*** $d_N$ ***in case of a communication range*** $R = 100m$ ***and a node density*** $\lambda = 0.05$ $nodes/m$

multi-hop-distance, by providing experimental results.

The effect of increasing the communication range R on the Gaussianity of the multi-hop-distance is found to be a deteriorating one since the distribution becomes more non-Gaussian for increasing communication ranges. The consistency between the experimental results and the approximations shows the accuracy of our kurtosis approximations. Figure 9(a) illustrates how the non-Gaussianity, of the multi-hop-distance is affected by the change in the maximum radial span R. This figure is obtained by using the Equation 28, hence it shows approximated values. The experimental results obtained for the effect of changing the radial span R on the kurtosis of the multi-hop-distance is illustrated in Figure 9(b). In both plots, the decrease in Gaussianity with increasing $R$ can be observed. Furthermore, for larger number of hops the multi-hop-distance distribution becomes more Gaussian.

An alternative way of investigating the similarity of a probability distribution to another one might be finding the mean square error between the values of these two distributions. Decreasing mean square error values between a Gaussian distribution and another distribution curve means an increasing Gaussian character. The mean square error (MSE) curves for changing node density and changing communication range are shown in Figure 10(a) and Figure 10(b), respectively. In these figures, the decaying nature of the non-Gaussianity for increasing number of hops is obvious. The MSE results are consistent with the results in Figures 8(a) and 9(a). In Figure 10(b), changing the $R$ values seems to have little effect on MSE, yet Gaussianity decreases for increasing $R$.

The approximation method for finding the kurtosis of the multi-hop distance is also found to be highly accurate as it can be observed in Figures 6 and 6.

The approximation method for finding the kurtosis of the multi-hop distance is also found to be highly accurate as

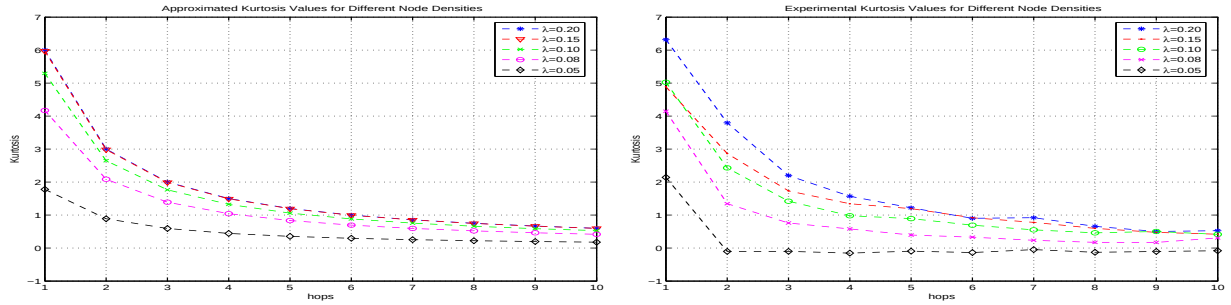


(a) *Approximate kurtosis of the multi-hop-distance* $\mathbf{d_N}$ *for different node densities.* $R = 100$.

(b) *Experimental kurtosis of the multi-hop-distance* $\mathbf{d_N}$ *for different node densities.* $R = 100$.

**Figure 8: Effect of Node Density on Gaussianity, Obtained by Experiments and Approximations**

it can be observed in Figures 6 and 6. The experimental and the approximated values of the kurtosis of the N-hop multi-hop processes, $N = 1, 2, 3, ..., 10$, are compared for four different node densities in Figure 6, whereas in Figure 6, the effect of changing the communication range R is shown. The graphs illustrate that the approximate results for the kurtosis of multi-hop-distance $\mathbf{d_N}$ are found to be similar to the results of the experiments.

# 5. DISCUSSION OF THE 2D CASE

The analysis in two dimensions is much more complicated than that of the linear case regarding the definition, modeling, and calculation of the expected distance and standard deviation values, which in turn makes it tedious to derive a general expression for the distributions in planar fields. Furthermore, the results of the linear process cannot be directly applied to the two dimensional case due to the geometric complexity of the planar case. In linear case, the pdf of a single hop is calculated considering the *vacant* regions and the *occupied* ones. For linear analysis, the definition of a *region* is a line segment, however for the analysis of the two dimensional case, the areas that are covered and those that are left vacant should be considered.

## 5.1 Planar broadcasts

For the purpose of investigating how planar hop distances are created, a sensor node may be selected as a reference point from which the distances are calculated. This sensor may be considered to broadcast packets, and these packets propagate radially outward. The maximum radius of the communication area of a sensor is $R$ and its coverage area is circular with a magnitude of $\Pi R^2$. The packets propagate hop by hop, where at each hop, a number of new sensors receive the broadcast packet. Therefore, at each hop a group of sensors that receive broadcast packets can be associated with that hop. Despite the fact that the sensors have radial communication areas, because of the random behavior of the node locations and due to a finite node density, these groups are not in the form of circular ring-shaped regions. In fact, they are regions with irregular shapes, which makes it difficult to model and analyze the planar process.

In Figure 13, the propagation of the broadcast hops can be observed to have non-circular boundaries. This irregular shape of the covered regions is caused by the randomness of the sensor nodes which are the centers of the disks of a particular hop. Each of the areas that are covered at a hop, but not covered by the previous hops is illustrated by a different color in Figure 13.

## 5.2 Directional propagation model

In order to address the need for eliminating the irregularity of areas, a geometric model for planar propagations, namely the *Directional Propagation Model* is proposed. The model consists of a series of angular coverage areas each limited by a fixed radius R, and a fixed angular span $\alpha$. Therefore, at each hop, an angular slice $S(\alpha, R)$ of a circular disk is covered. This area is analogous to the line segment of length R in case of linear propagation. Figure 14 shows the model. At each hop, the aim is to find the farthest point that can be reached within this angular communication range. For instance, at hop $i$, within the $S(\alpha, R)$ coverage area of node $P_{i-1}$, node $P_i$ is selected in a way such that it is maximally distant from the point $P_{i-1}$. The central axis of the slice $S(\alpha, R)$ divides the area into two regions with equal areas by dividing the angle $\alpha$ into two parts with angles $\frac{\alpha}{2}$. The axis is always taken to be parallel to a line connecting the source node and a target point. A chain of such slice-regions forms a series of hops, which forms the multi-hop-distance. As it was the case for the linear analysis, a single-hop-distance is crucial for modeling the multi-hop-distance distribution. For this reason, the following discussion is based on a single-hop-distance in two dimensions.

## 5.3 Single-hop-distance in two dimensions

As it is mentioned in the previous section, the single-hop-distance is analyzed in order to find an expression that models the multi-hop-distance distribution. Analogous to the linear single-hop-distance analysis, at each hop the maximum coverage area is composed of a vacant region created by the previous hop and another vacant region created by the current hop. In other words, at each hop, the sensor node with the maximum distance to the *tip* of the circular slice $S(\alpha, R)$ is searched within the coverage area.

## 5.4 Unit area definitions and geometric approximations

The following are the definitions of the areas used in this discussion and shown in Figure 14. $P_i$ is the point chosen at hop $i$ and $r_i$ is the distance between $P_i$ and $P_{i-1}$. The area covered at hop $i$ is denoted by $A_i$ which is equal to

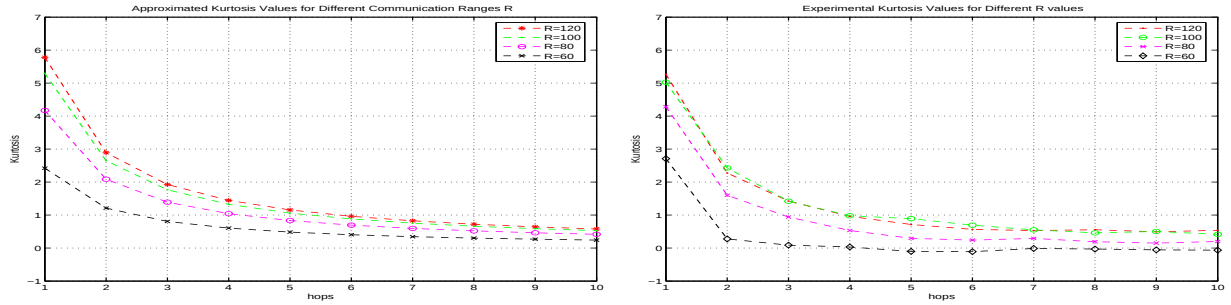


(a) *Approximated kurtosis of the multi-hop-distance* $\mathbf{d_N}$ *for different values of range* $R$. $\lambda = 0.1$. (b) *Experimental kurtosis of the multi-hop-distance* $\mathbf{d_N}$ *for different values of range* $R$. $\lambda = 0.1$.

**Figure 9: Effect of Communication Range on Gaussianity, Obtained by Experiments and Approximations**

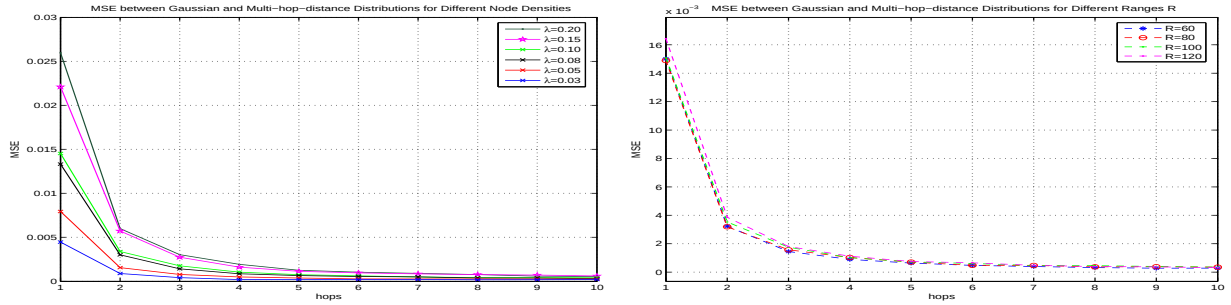


(a) *Mean square error between the experimental Gaussian distribution and the distribution of the multi-hop-distance for different node density values.* $R = 100$. (b) *Mean square error between the experimental Gaussian distribution and the distribution of the multi-hop-distance for different ranges.* $\lambda = 0.1$.

**Figure 10: Mean Square Error between experimental Gaussian distribution and Multi-hop-distance distribution**

$\frac{\alpha}{2} {r_i}^2$. Furthermore, $A_{e_{i-1}} \cong \frac{\alpha}{2}\left(R^2 - {r_{i-1}}^2\right)$ denotes the vacant area of hop $i$. $A_{e_{i-1}}$ is an approximation to the area of a ring slice. For smaller values of the angular span $\alpha$ and the radial span $R$, the approximation improves and becomes more accurate.

## 5.5 Distribution of distance

The distribution function of the linear single-hop-distance is obtained by conditional probabilities. The pdf of the traveled region in a hop is calculated, given that the previous hop has left a certain amount of vacancy in its own coverage region. In case of planar single-hop-distance, the pdf of the distance traveled can be obtained in a similar way. This time, the pdf of the region covered at the current hop is found given that the previous hop has left a certain area as a vacant region. As the regions can solely be defined by their radial spans while having their angular spans constant, a relation between the areas and the radii can be established. This leads to determining the pdf of the one-hop-distance, since there exists a one-to-one matching between an area and a radius. According to our Directional Propagation Model, the probability distribution function of distance traveled at a hop is found as follows:

$$f\left(r_i\right) = \frac{\alpha r_i \sigma e^{-\sigma \frac{\alpha}{2}\left[2Rr_i - {r_i}^2\right]}}{e^{-\sigma \frac{\alpha}{2} R^2} \int_{R-r_{i-1}}^{R} \alpha r_i \sigma e^{\sigma \frac{\alpha}{2}(R-r_i)^2} dr_i} \qquad (32)$$

The integral in the denominator of this function designates the scaling factor caused by the condition that the distance $r_i$ can only be found within the radial range $(R - r_{i-1}, R)$. The numerator along with the factor $e^{-\sigma \frac{\alpha}{2} R^2}$ in the denominator, is the probability that the furthest node that can be reached within the coverage area is $r_i$ away from point $P_{i-1}$.

The expectation and standard deviation of single-hop-distance in two dimensions are then calculated using Equation 32 and they are used to obtain expressions to evaluate the multi-hop-distance distribution. Our directional motion model serves to establish an analogy between the one dimensional analysis and the two dimensional analysis by introducing the concept of *angular slice*. An angular slice region $(S(\alpha, R))$ is the analogy of the linear coverage length $R$ in linear analysis. In this way, the complexity of the regions formed by broadcast cycles is avoided. The detailed analysis in two dimensions is left as a future study.

# 6. CONCLUSION

In this paper, the probability distribution of the maximum Euclidean distance for a given hop distance is inspected in case of a linear sensor network with uniform distribution of sensors. The distribution of the single-hop-distance is obtained in terms of the mean and the standard deviation of the distance. An approximation for these values of a single-

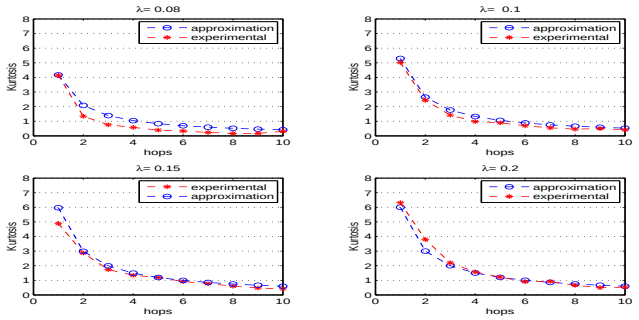


**Figure 11:** ***Comparison of the experimental and the approximated kurtosis of the multi-hop-distance*** $\mathbf{d_N}$ ***for different values of node density.***

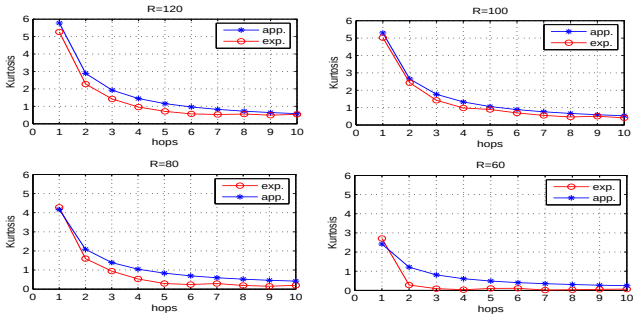


**Figure 12:** ***Comparison of the experimental and the approximated kurtosis of the multi-hop-distance*** $\mathbf{d_N}$ ***for different values of communication range.***

hop-distance is used to derive approximation expressions for the multi-hop-distance. Additionally, the similarity between the multi-hop-distance distribution and the Gaussian distribution is inspected. A statistical measure called "kurtosis" is used for this purpose. An effective way of approximating the kurtosis formula for multi-hop-distance is derived.

Due to the computational cost of theoretical expressions, which limit the number of hops in multi-hop analysis, highly effective and accurate approximations are formalized to obtain results for high number of hops. Furthermore, experiments are conducted for the purpose of evaluating the validity of the derived theoretical expressions and our approximations for these expressions. The approximations and the numerical results of the theoretical expressions are found to be highly consistent with the experimental results. Finally, a discussion on the creation of hop distances in planar networks and the complexity of the distance-hop relation in two-dimensions is provided.

Further work is required to inspect the applicability of our methods to linear sensor networks with non-uniform node distributions and with sensors of variable communication ranges. Moreover, finding effective models to be applied to planar sensor networks is identified as a future study.

## 7. ACKNOWLEDGMENT

The authors would like to thank Serhan Ziya for fruitful discussions at the early stages of this work.

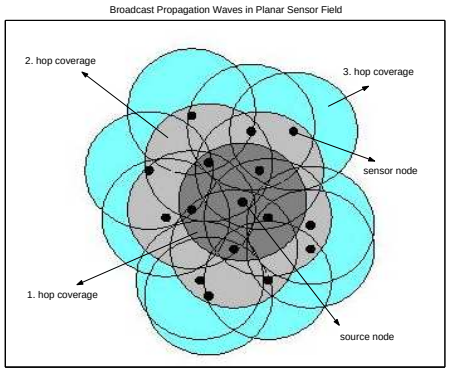


**Figure 13:** ***Coverage areas of planar broadcast propagation for 3 hops***

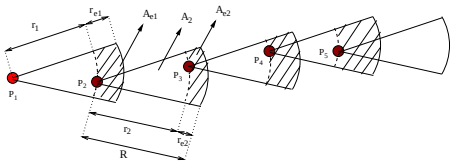

**Figure 14:** ***Directional Propagation Model to illustrate the propagation of broadcasts in a planar network. At each step, the farthest point that is inside the communication area (a disk slice) is selected as the next transmitter. In this figure, only these farthest points are shown.***

## 8. REFERENCES

[1] Y. Cheng and T. Robertazzi. Critical connectivity phenomena in multihop radio models. *IEEE Transactions on Communications*, 37:770–777, July 1989.

[2] A. Hyvärinen, J. Karhunen, and E. Oja. *Independent Component Analysis*. John Wiley & Sons, 2001.

[3] G. Korkmaz, E. Ekici, F. Ozguner, and U. Ozguner. Urban multi-hop broadcast protocols for inter-vehicle communication systems. In *Proceedings of First ACM Workshop on Vehicular Ad Hoc Networks (VANET 2004)*, pages 76–85, October 2004.

[4] R. Nagpal, H. Shrobe, and J. Bachrach. Organizing a global coordinate system from local information on an ad hoc sensor network. In *2nd International Workshop on Information Processing in Sensor Networks (IPSN '03)*, April 2003.

[5] D. Niculescu and B. Nath. Ad hoc positioning system (aps). In *IEEE GlobeCom*, November 2001.

[6] D. Niculescu and B. Nath. Dv based positioning in ad hoc networks. *Telecommunication Systems*, 22(1-4):267–280, 2003.

[7] C. Savarese, J. Rabay, and K. Langendoen. Robust positioning algorithms for distributed ad-hoc wireless sensor networks. In *Proceedings of the General Track: 2002 USENIX Annual Technical Conference*, pages 317–327, 2002.

[8] S. Vural and E. Ekici. Wave addressing for dense sensor networks. In *Proceedings of Second International Workshop on Sensor and Actor Network Protocols and Applications (SANPA 2004)*, pages 56–66, August 2004.